13th World Conference on Earthquake Engineering
Vancouver, B.C., Canada
August 1-6, 2004
Paper No. 113

ANALYTICAL AND EXPERIMENTAL SEISMIC ASSESSMENT OF IRREGULAR RC BUILDINGS

Seong-Hoon JEONG[1] and Amr S. ELNASHAI[2]

SUMMARY

Seismic assessments of irregular buildings need special attention while regular structures can be readily idealized and assessed using 2D conventional methods. In this paper, an advanced analytical assessment methodology for irregular buildings is presented. In the proposed method, 3D modeling is utilized to capture the torsional and bi-directional response of the irregular buildings. A layering technique, termed Planar Decomposition, is proposed and shown to furnish detailed information on the demand and capacity of critical members. As an application, an irregular 3D structure intended for a full-scale experimental testing at the Joint Research Center, Ispra, Italy under the auspices of the EU project Seismic Performance Assessment and Rehabilitation (SPEAR) is assessed using the advanced methodology. Through its application to the test structure and comparison to the conventional methods, it is shown that normal assessment procedures may be inaccurate and even unconservative, in terms of the performance assessment of irregular buildings. This highlights the importance of monitoring the damage state on a member-by-member basis instead of a story or structure level as well as the significance of including torsional effect in the assessment procedure.

INTRODUCTION

Earthquake field investigations repeatedly confirm that irregular structures suffer more damage than their regular counterparts. This is recognized in seismic design codes, and restrictions on abrupt changes in mass and stiffness are imposed. Irregularities in dimensions affect the distribution of stiffness, and in turn affect capacity, while mass irregularities tend to influence the imposed demand. Elevation irregularities have been observed to cause storey failures due to non-uniform distribution of demand-to-supply ratios along the height. Plan irregularities, on the other hand, cause non-uniform demand-to-capacity ratios amongst the columns within a single floor. Quantitative measures of seismic assessment on a floor-by-floor basis have been used for many years, in the form of storey drift ratios that provide a single number that portrays the demand-to-supply picture along the height of a structure. Quantitative, readily available

[1] Ph.D. Candidate, Department of Civil and Environmental Engineering, University of Illinois at Urbana-Champaign; Research Assistant, Mid-America Earthquake Center, Email: sjeong1@uiuc.edu
[2] Willett Professor of Engineering, Acting Director of Mid-America Earthquake Center, Department of Civil and Environmental Engineering, University of Illinois at Urbana-Champaign, Email: aelnash@uiuc.edu

and verified measures of demand-to-capacity ratios over the plan of a structure subjected to bidirectional transient dynamic loading and responding in the inelastic range are still lacking. In this paper, an analytical index is derived based on generic response characteristics. The index accounts for the multi-directionality of earthquake motion as well as the asymmetry of the structure; hence it captures the true three-dimensional inelastic effects that govern the response of RC structures. The adoption of such a damage measure opens to door to the derivation of spatial fragility curves and surfaces.

EXISTING DAMAGE INDICES

The importance of an appropriate damage index as a means of limit state characterization to assess the status of structures is shown by Bento and Azevedo [1]. Two significant reviews of damage indices were conducted by Williams and Sexsmith [2] and by Ghobarah *et al*. [3]. Damage indices may be sub-divided into three groups: non-cumulative, cumulative, and combined. The response parameters used to classify the three types of damage indices are the maximum deformation, the hysteric behavior or fatigue, and the deformation and energy absorption. The Park and Ang [4] index is widely used in the literature owing to its calibration to a number of experimental programs. From a practical point of view, the deformation-based non-cumulative damage index may be meaningful enough, taking into account that few earthquakes apply a large number of cycles to structures in the conventional period range. Moreover, according to Williams and Sexsmith [2] and Kappos and Xenos [5], adding the energy component to the index may be insignificant. Additionally, a deformation-based non-cumulative damage index has the advantages of simplicity in calculations, while the combined damage index necessitates calibrations to determine its empirical parameters.

The overall damage state should be determined when assessing the seismic performance of a structure. Williams and Sexsmith [2] divided global damage indices into two groups: (a) weighted average indices and (b) measures based on modal parameters. Weighted average indices have been presented by Park and Ang [6], Park, Ang and Wen [7], Chung *et al*. [8, 9], Kunnath *et al*. [10, 11] and Bracci *et al*. [12]. On the other hand, Roufaiel and Meyer [13], DiPasquale and Cakmak [14, 15] and DiPasquale *et al*. [16] presented damage measures based on modal parameters.

Whereas existing damage indices present many choices for the analyst, their applicability is restricted to local and 2D global assessments, as shown in Figure 1.

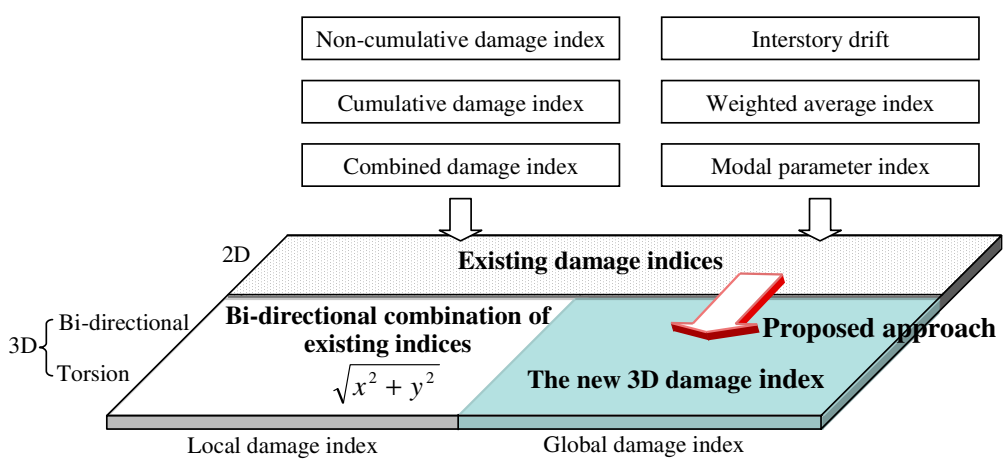

Figure 1 Monitoring scopes of damage indices

For the seismic assessment of structures with plan irregularities, a damage index should be able to reflect 3D structural behavior such as torsion and bi-directional response. For the assessment of hybrid (e.g. frame-wall) structures, an approach that combines various damage indices is needed because different

damage indices should be used according to the types of structural subsystems. Moreover, the choice of a suitable damage index depends on the assessment limit state of interest and effect of non-structural components (Colangelo [17]). The abovementioned brief review of existing damage indices, and additional requirements not covered by existing measures, highlight the necessity of developing a versatile damage assessment method applicable to 3D global assessment of irregular structures. The new approach is described in the subsequent sections. A treatment of the basis for the procedure, termed planar decomposition is depicted and thereafter, the various steps of the procedure are developed. The application example given confirms that the new damage index represents the response of complex 3D structures.

NEW DAMAGE MONITORING PROCEDURE

Planar decomposition

Torsion causes variations in column drift. Therefore using the conventional 2D damage index is inadequate when monitoring the damage of a building exhibiting torsional response. For example, interstory drift cannot capture the localized variation in demand because the drift of columns varies according to their position in-plan. In order to conduct accurate damage assessment of buildings exhibiting torsion, a new method termed Planar Decomposition is proposed herein. In the proposed method, the whole structure is decomposed into planar frames that are considered to be the basic elements of lateral resistance, as shown in Figure 2.

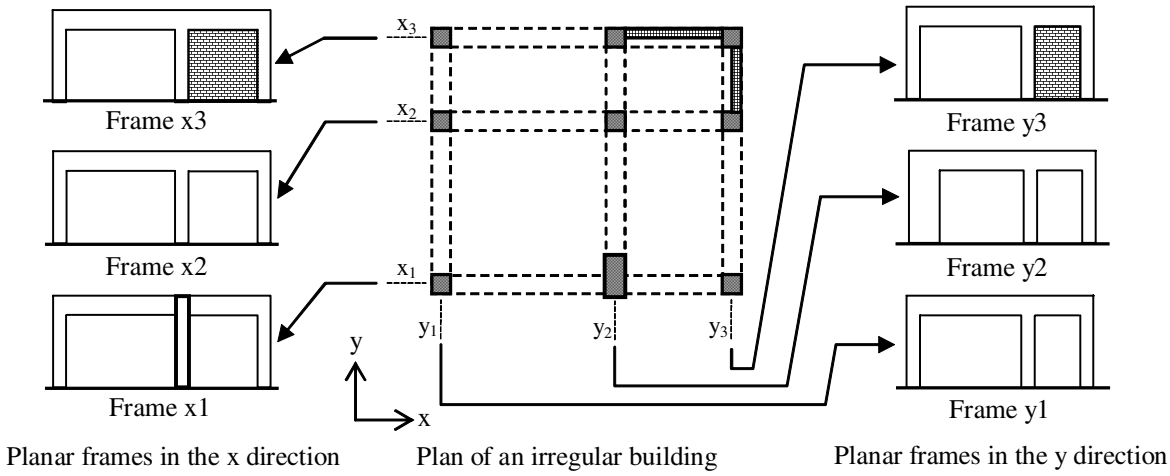

Figure 2 Concept of the proposed method

Analysis features such as material modeling, assumptions in member dimensions, connection modeling, and even numerical algorithms of analysis programs affect the ensuing result. Because of the sensitivity of analytical assessment, defining demand-only limit state is uncertain and the ensuing measures may vary significantly when the above analysis parameters are varied. Therefore, in order to provide a more robust damage assessment procedure, the demand-to-capacity ratio (DCR) is used in this paper to define limit states.

Capacities and demands of individual planar frames are obtained by static pushover analyses and dynamic time history analyses, respectively. By dividing the demand by the capacity, the DCR of each planar frame is calculated. DCRs of individual planar frames are combined for the assessment of the whole structure. Unidirectional DCR of the whole structure is calculated by weighted combination of DCRs of planar frames and implementation of damage localization. Finally, unidirectional DCR of the structure in two orthogonal directions are combined to form a single value of bidirectional DCR of the whole structure.

Unidirectional demand-to-capacity ratio

The capacity of each planar frame is obtained from 2D static pushover analysis of an individual planar frame. The displacement capacity is that corresponding to $0.85P_i$ where the strength drop is 15% of its maximum value P_i. This is not an integral part of the new procedure, but can be decided by the analyst. Through the above procedure, a set of decomposed 2D capacities (u_{x1}, u_{x2}, u_{x3}, u_{y1}, u_{y2} and u_{y3}) is prepared to calculate the demand-to-capacity ratios (DCRs) of planar frames. The subscripts represent frame identifications, as shown in Figure 2. By monitoring the maximum unidirectional displacement of each planar frame, a set of decomposed 2D demands (Δ_{x1}, Δ_{x2}, Δ_{x3}, Δ_{y1}, Δ_{y2} and Δ_{y3}) is obtained.

The DCR of each planar frame is calculated by dividing the displacement demand by the ultimate displacement capacity as shown in Eq. (1). The DCR of each planar frame is scaled by using a weighting parameter, defined as W_{xi} or W_{yj} (Eq. 2), and then combined into a single damage index in each direction as given in Eq. (3). The subscript x and y represent the directions of frames and i and j represent the frame identification numbers. The weighting parameter of each planar frame in Eq. (2) represents the drift capacity contribution of the planar frame to the total drift capacity of the structure. The weighting parameter can be determined by the analyst according to the purpose of the assessment.

$$DCR_{xi} = \Delta_{xi} / u_{xi}, \qquad DCR_{yj} = \Delta_{yj} / u_{yj} \tag{1}$$

$$W_{xi} = u_{xi} / \sum_{i=1}^{m} u_{xi}, \qquad W_{yj} = u_{yj} / \sum_{j=1}^{n} u_{yj} \tag{2}$$

$$\overline{DCR}_x = \sum_{i=1}^{m} (W_{xi} \cdot DCR_{xi}), \quad \overline{DCR}_y = \sum_{j=1}^{n} (W_{yj} \cdot DCR_{yj}) \tag{3}$$

in which Δ_{xi} is the demand of frame xi, u_{xi} is the capacity of frame xi, Δ_{yj} is the demand of frame yj and u_{yj} is the capacity of frame yj. m and n are total numbers of planar frames in x and y direction, respectively.

$\overline{DCR}_x$ and $\overline{DCR}_y$ represent the unidirectional drift demand-to-capacities of the structure as simple linear combinations of individual planar frame DCRs. Using these absolute sums of planar frame DCRs with the DCR of a critical frame, the effect of the damage concentration features in the final calculation of the unidirectional structure DCRs as shown in Eq. (5) and Eq. (6).

The critical frame is that which suffers the highest demand-to-capacity ratio and it is determined by investigating the maximum DCR of all planar frames. The maximum DCRs are obtained by Eq. (1). However, in many cases, the critical frame can be determined easily without recourse to the above approach. If the eccentricity of the plan is large, the furthest frame from the center of rigidity is the critical frame. In the case of small eccentricity, the frame that has the lowest capacity is the critical frame.

Effect of torsion on the demand-to-capacity ratio of the critical frame can be determined by the drift demand at a standard point (O_x or O_y) and the angle of torsion (θ), as shown in Figure 3. The standard point can be any point on the plan, because the effect of its location on the capacity of the critical frame is automatically reflected by the distance (λ_x or λ_y) between the standard point and the critical frame, as shown in Eq. (4). The reduced drift capacities of critical frames (u_{xr} and u_{yr} in Figure 3) can be calculated by Eq. (4).

$$u_{xr} = u_{xcr} - \theta \times \lambda_x \qquad u_{yr} = u_{ycr} - \theta \times \lambda_y \tag{4}$$

in which u_{xcr} and u_{ycr} are the drift capacities of the critical frames in the x and y directions, respectively and they are determined by 2D static pushover analysis of each critical frame. θ is the angle of torsion, and λ_x and λ_y are the distances between the standard point and the critical frame.

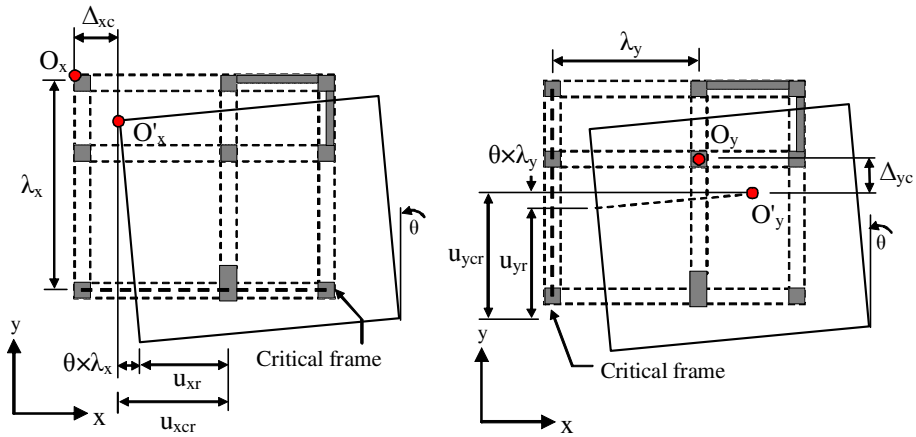

(a) x direction planar frames (b) y direction planar frames

Figure 3 Effect of torsion on the critical frame

Eq. (5) is derived to enhance the effect on the DCR_{xcr} of the critical frame as its damage becomes more severe. As the critical frame approaches failure, its DCR approaches unity.

$$DCR_x = (u_{xr} - \Delta_{xc}) / u_{xr} \cdot \overline{DCR}_x + \frac{\Delta_{xc}}{u_{xr}} DCR_{xcr} \tag{5}$$

in which Δ_{xc} is x direction drift demand at the standard point (O_x), DCR_{xcr} is the DCR of the critical frame. Similarly, the DCR in the y direction can be calculated as shown in Eq. (6).

$$DCR_y = (u_{yr} - \Delta_{yc}) / u_{yr} \cdot \overline{DCR}_y + \frac{\Delta_{yc}}{u_{yr}} DCR_{ycr} \tag{6}$$

Bidirectional demand-to-capacity ratio

The demand-to-capacity ratios (DCR_x and DCR_y) in two orthogonal directions are combined to determine the overall DCR. The method of combination is presented in Figure 4. The combined capacity of x and y directions is assumed to be an ellipse, which is a second order function of the variation between two unidirectional capacities. These two unidirectional capacities are x direction-only capacity (d_{ux}) and y direction-only capacity (d_{uy}), as shown in Figure 4.

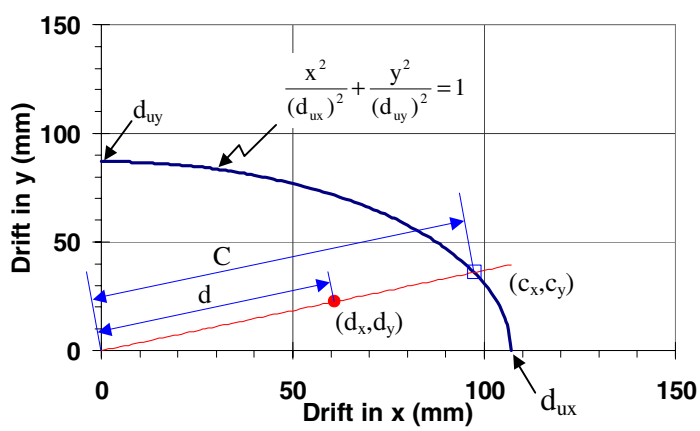

Figure 4 Bidirectional demand and capacity

The unidirectional capacities (d_{ux} and d_{uy}) are obtained from the 2D pushover analyses of the 3D structure in the x and y directions, respectively. The originally 3D structure is temporarily restrained in the out-of-

plan direction for conducting the 2D pushover analysis to obtain pure 2D unidirectional capacities. Therefore, in order to use the bidirectional capacity relationship (Figure 4) defined by d_{ux} and d_{uy}, the demand-to-capacity ratios (DCR_x and DCR_y) as calculated in Eq.s (5) and (6) should be converted into equivalent demand (d_x and d_y) in 2D, as shown in Eq. (7). The bidirectional demand is defined as the distance between the origin (0, 0) and the point (d_x, d_y) and it is obtained by Eq. (8).

$$d_x = DCR_x \cdot d_{ux}, \qquad d_y = DCR_y \cdot d_{uy} \tag{7}$$

$$d = \sqrt{(d_x)^2 + (d_y)^2} \tag{8}$$

In Figure 4, the ratio of the drift in y direction to the drift in x direction defines a line the slope of which is $s=d_y/d_x$. The intersection of the latter line and the ellipse shown in Figure 4 represents the bidirectional capacity of the structure. The bidirectional capacity is calculated as the distance from the origin (0, 0) to the intersection point (C_x, C_y) as calculated in Eq. (9). Once the equations of the line and the ellipse are determined, the coordinates of the intersection point C_x and C_y can be calculated as shown in Eq. (10).

$$C = \sqrt{(C_x)^2 + (C_y)^2} \tag{9}$$

$$C_x = \sqrt{\frac{(d_{ux})^2 (d_{uy})^2}{s^2 \cdot (d_{ux})^2 + (d_{uy})^2}}, \qquad C_z = \sqrt{\frac{s^2 \cdot (d_{ux})^2 (d_{uy})^2}{s^2 \cdot (d_{ux})^2 + (d_{uy})^2}} \tag{10}$$

The combined DCR is a ratio of the demand d from Eq. (8) to the capacity C from Eq. (9). The combined DCR is calculated by DCR_x and DCR_y with scaling factors a_x and a_y, as shown in Eq. (11).

$$DCR = \frac{d}{C} = \sqrt{a_x \cdot (DCR_x)^2 + a_y \cdot (DCR_y)^2} \tag{11}$$

in which a_x and a_y are

$$a_x = \frac{s^2 \cdot (d_{ux})^2 + (d_{uy})^2}{(1+s^2) \cdot (d_{uy})^2}, \qquad a_z = \frac{s^2 \cdot (d_{ux})^2 + (d_{uy})^2}{(1+s^2) \cdot (d_{ux})^2} \tag{12}$$

SAMPLE APPLICATION

Description of the example structure

In order to demonstrate the applicability of the proposed methodology, the DCR of a three-story, 2×2 bay RC frame with asymmetric plan is calculated. The structure was designed for a full-scale pseudo-dynamic test at the Joint Research Center, Ispra, Italy under the auspices of the EU project Seismic Performance Assessment and Rehabilitation (SPEAR). Further details on the test are given in Negro *et al.* [18] and Molina *et al.* [19]. The test building has been designed to gravity loads alone, using the concrete design code applied in Greece between 1954 and 1995. It was built with the construction practice and materials used in Greece in the early 70's. The structural configuration is also typical of non-earthquake-resistant construction of that period. Infill walls and stairs are omitted in the test structure. Layout of the test structure is represented in Figure 5. The large column (C6) in Figure 5 (b) provides the whole structure with more stiffness and strength in the y direction than in the x direction. Hereafter the large column is referred to C6 while strong and weak directions are referred to as y and x directions, respectively. The thickness of slab is 150 mm and total beam depth is 500 mm. The sectional dimension of C6 is 750×250 mm whereas all other columns are 250×250 mm. The structure is a strong-beam weak-column frame building and the second story is the weak story. Detailed descriptions on the test structure and its analytical modeling are given in Jeong and Elnashai [20].

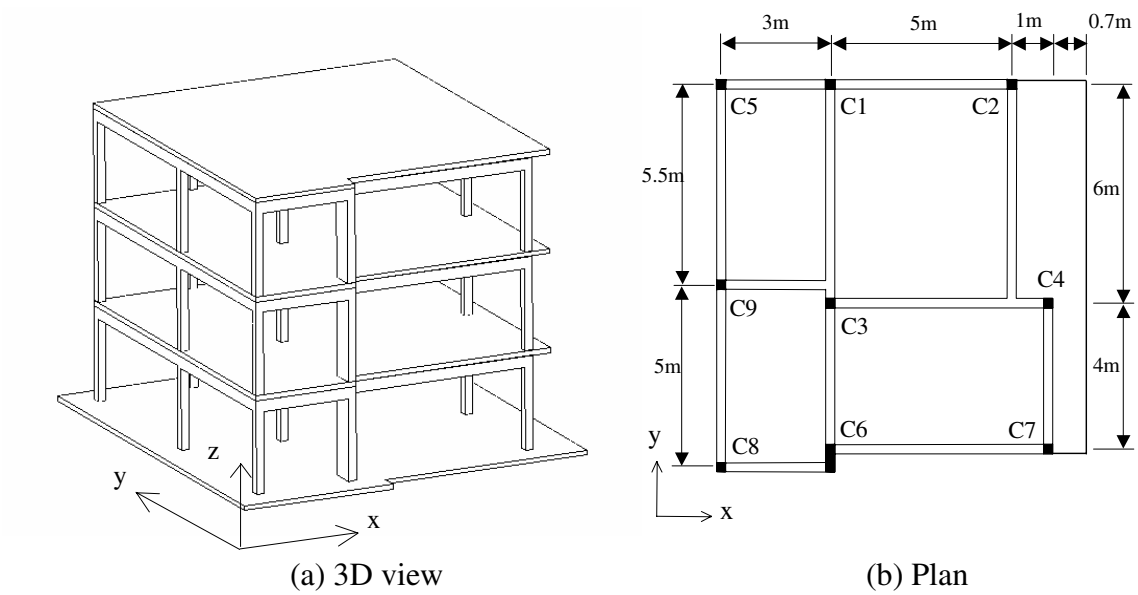

(a) 3D view (b) Plan

Figure 5 SPEAR test structure

Application of the planar decomposition and capacity calculation

Since the collapse of a single story means the collapse of the whole structure, in this paper, damage assessment is conducted with the critical story which is the second story for the SPEAR structure (Jeong and Elnashai [20]).

The locations and directions of the planar frames as the basic elements of the lateral resistance system are represented in Figure 6. To determine the capacities, static pushover analyses are performed for the individual planar frames and the critical story as a whole, as shown in Figure 7 and Figure 8. The pushover curves of planar frame y2 (Figure 7 (b)) and the second story (Figure 8 (b)), a large difference in strength was observed according to the sign of loading. In the positive y direction, the concrete in the section of C6 is in tension and the contribution of the concrete to the structure does not exist. However, under the negative y direction loading, the large column C6 is in compression and concrete in the section fully resists the external forces.

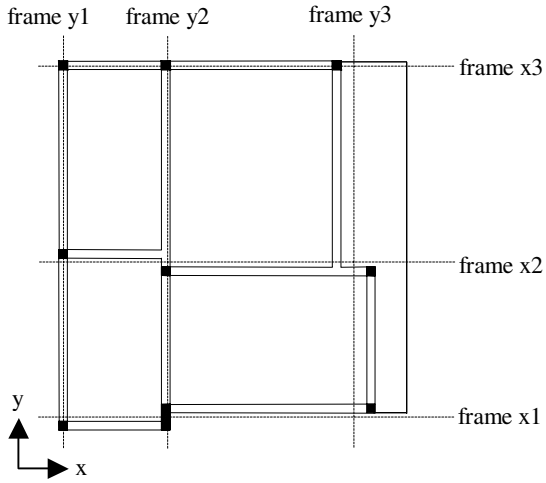

Figure 6 Frame lines on the plan of the example structure

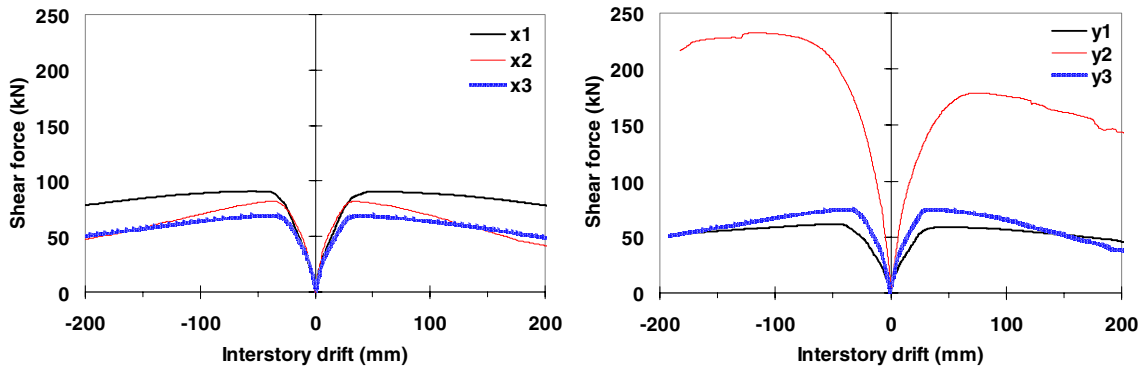

(a) x directional loading (b) y directional loading

Figure 7 Pushover curves of planar frames at the second story

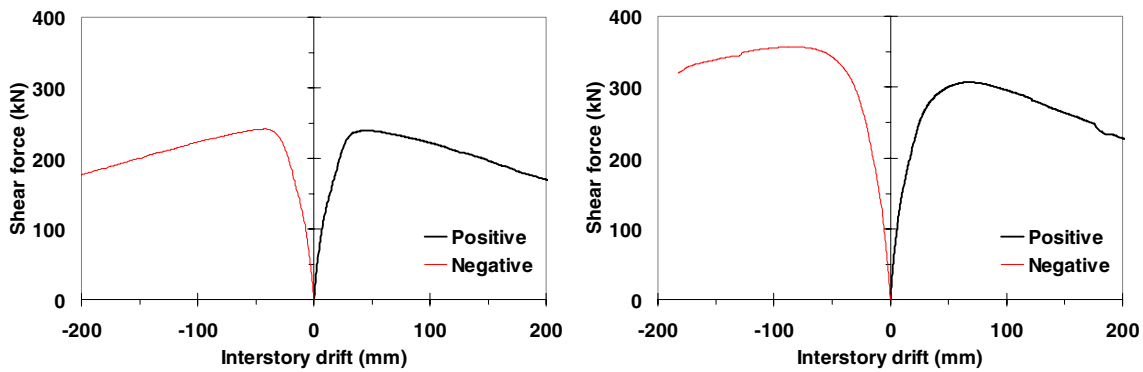

(a) x directional loading (b) y directional loading

Figure 8 Pushover curves of the second story

The ultimate deformation capacity is defined as the interstory drift when the actual final collapse occurs and it was assumed to be the point where the force reaches at 85% of its maximum force after the peak. If the latter point cannot be determined from the pushover curves, another definition is utilized for the ultimate deformation. According to FEMA 356 [21], the interstory drift for collapse prevention limit state of RC frames is 4% of the story height. Assuming the collapse prevention limit is at a damage index of 0.6, as suggested by Ghobarah, et al. [3], the ultimate interstory drift can be calculated by extrapolating the collapse prevention limit (4% interstory drift) by the ratio of final collapse damage index to collapse prevention damage index (1.0/0.6). Therefore, multiplying 4% by (1.0/0.6) gives the ultimate interstory drift of 6.7% of the story height. Table 1 represents the calculated capacities of planar frames and the critical story. V_p in the table represents peak shear force.

Table 1 Ultimate deformation capacities of planar frames and the critical story

Directions	Frames	Ultimate interstory drift (mm)			
		Positive direction		Negative direction	
x direction	x1	201	6.7% story height	-201	6.7% story height
	x2	99	Displ. at 0.85 V_p	-101	Displ. at 0.85 V_p
	x3	138	Displ. at 0.85 V_p	-136	Displ. at 0.85 V_p
	Whole story	137	Displ. at 0.85 V_p	-139	Displ. at 0.85 V_p
y direction	y1	154	Displ. at 0.85 V_p	-175	Displ. at 0.85 V_p
	y2	176	Displ. at 0.85 V_p	-129	Displ. at 0.85 V_p
	y3	108	Displ. at 0.85 V_p	-119	Displ. at 0.85 V_p
	Whole story	154	Displ. at 0.85 V_p	-182	Displ. at 0.85 V_p

Damage assessment and comparison

Experimental results

For the SPEAR test, two orthogonal components of the semi-artificial record which was modified based on the record of Montenegro 1979 (Herceg Novi) were applied to the structure bi-directionally. Two main tests were performed with different intensities of ground acceleration. The first test was performed with PGA of 0.15g and followed by the second test with PGA of 0.20g. The experimental results are presented in Figure 9.

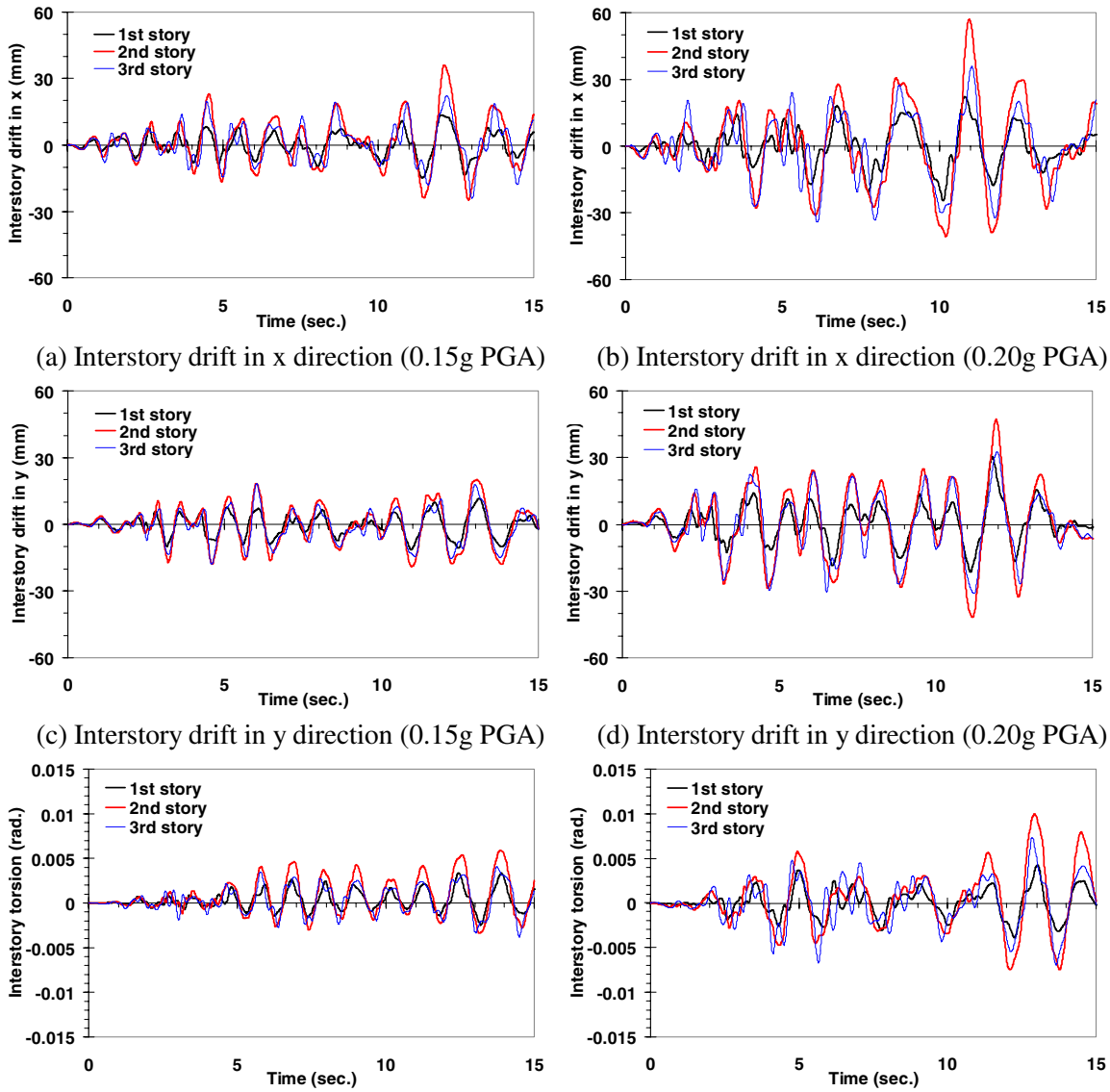

(a) Interstory drift in x direction (0.15g PGA)

(b) Interstory drift in x direction (0.20g PGA)

(c) Interstory drift in y direction (0.15g PGA)

(d) Interstory drift in y direction (0.20g PGA)

(e) Interstory torsion (0.15g PGA)

(f) Interstory torsion (0.20g PGA)

Figure 9 Experimental results of the SPEAR test

Calculation of damage index

The most widely used deformation based damage index is the ratio of maximum interstory drift (ID) demand to the ultimate interstory drift capacity. As a damage index of 3D structures, the interstory drift (ID) has often been considered to be the mean value of interstory drifts (IDs) at all column locations in the

story. The comparisons of the mean value of IDs at all column locations in the second story and ID at the center of mass (COM) from the 0.20g PGA experimental results are presented in Figure 10. Since the difference between two kinds of ID is negligible, ID at COM is utilized as a conventional damage index in this paper.

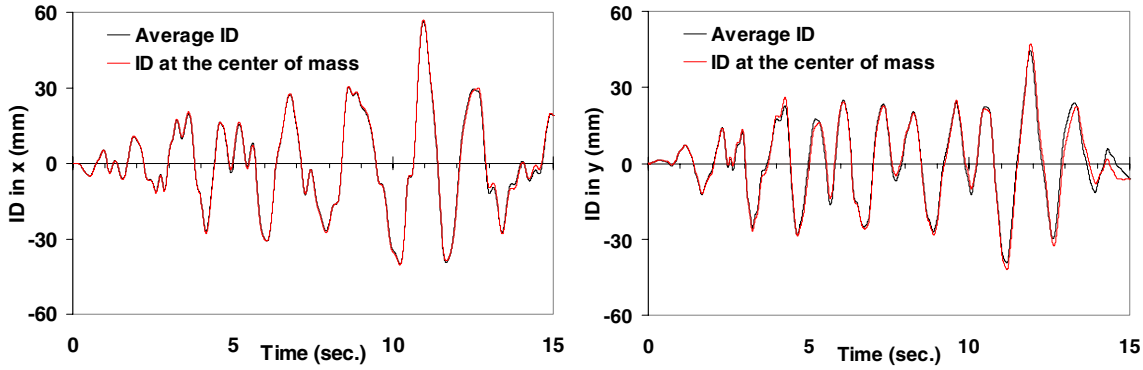

(a) x direction (b) y direction

Figure 10 Comparison of the average ID and ID at the center of mass (2nd story, 0.20g PGA)

The proposed 3D damage index is calculated using the experimental results presented in Figure 9. And it is compared with the 2D conventional damage index which is the ratio of maximum interstory drift at COM to the corresponding ultimate deformation capacity in the weak direction, as shown in Figure 11. The difference between the proposed 3D damage index and the 2D conventional damage index becomes larger when the torsional response is significant. Even when the interstory drift at the center of mass is zero, the deformation at flexible edge columns can be significant due to torsion. This situation is reflected by the proposed damage index in Figure 11; the 3D New damage index shows significant damage level even when the 2D conv. damage index is zero.

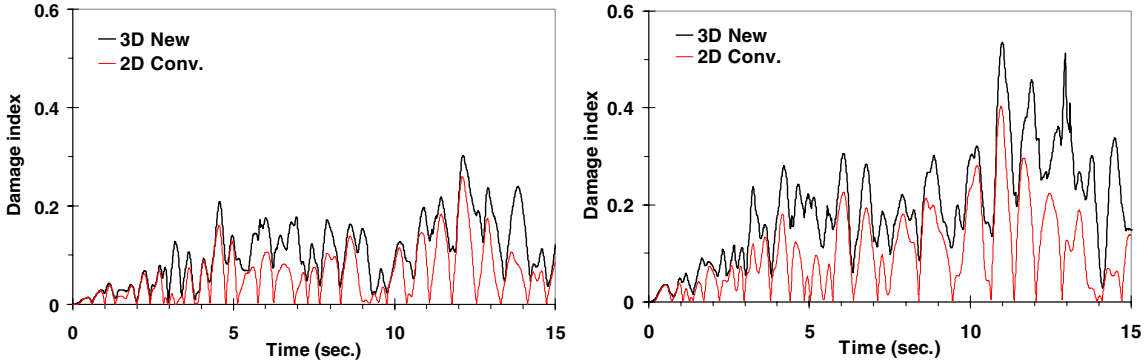

(a) 0.15g PGA (b) 0.20g PGA

Figure 11 Comparison of the proposed damage index and the conventional damage index

Damage assessment

While it was shown that the proposed damage index is sensitive to torsional effect on the damage of the structure, an appropriate scale of damage level should be provided for the use of the damage index to be effective. There are several references that have defined limit states signifying levels of damage and presents limit states in the format of the interstory drift ratio which is the ratio of interstory drift to the story height. However the presented values in the latter references cannot directly be applied to the test structure in this paper. The limit states by Ghobara et al. [3] were obtained from the probabilistic response of structures of which the characteristics were determined by Monte Carlo simulation. The mean value of the maximum ID used in Ghobara et al. [3] is compared with the experimental result of the SPEAR test

structure in Figure 12. There are large differences between the two response. From the statistical point of view, the SPEAR test structure is a point at the tail of the probability distribution and its response is far from the mean value of responses simulated in Ghobara et al. [3].

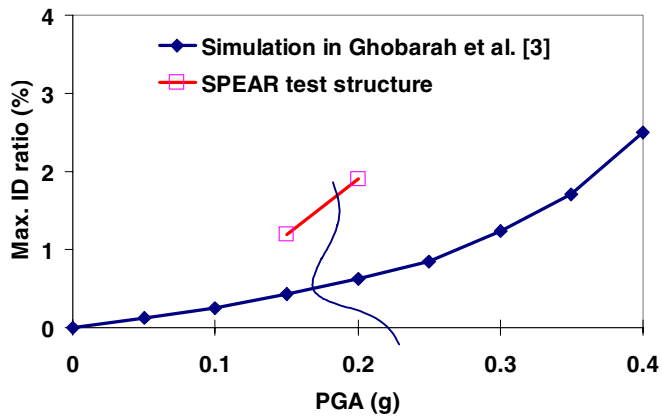

Figure 12 Mean value of the maximum ID (for the existing frame, soil site) used in Ghobara et al. (1998) and the experimental results of the SPEAR frame

Levels of damage and the corresponding interstory drifts used in this paper are presented in Table 2. (+) and (-) in the table represent positive direction and negative direction, respectively. Elastic limit and collapse point can be determined from the pushover curves in Figure 8 and Table 1. The intermediate limit states are defined based on the damage levels in Ghobara et al. [3]. They are obtained by extrapolating the elastic limit under the assumption that the damage level after yielding point is directly related to the ductility demand. The damage index is defined by the percentage ratio of ID to the story height in Ghobara et al. [3]. Here, only the ductility (ratio of max. ID to elastic limit) relationship was adopted to obtain the limit states for the SPEAR test structure, as represented in Table 2. In Table 3, the damage indices correspond to each damage level is calculated by dividing the interstory drifts by the collapse deformation. Taking the average of the latter damage indices in all directions, the limit states for damage index for the damage assessment of the SPEAR structure are calculated, as presented in Table 3.

Table 2 Damage levels and the corresponding interstory drifts (ID)

References	Damage levels			Interstory drifts (mm)			
		Limit states	ID/ Δy	x (+)	x (-)	y (+)	y (-)
Ghobarah *et al*. [3]	No damage	Elastic limit	1.0	28	27	32	34
	Minor damage	2 × Elastic limit	2.0	56	54	64	68
	Repairable damage	4 × Elastic limit	4.0	112	108	128	136
Pushover analysis	Collapse	Δ at $0.85V_p$		137	139	154	182

Table 3 Damage levels and the corresponding damage indices (D.I.)

Damage levels	Interstory drifts (ID), Damage indices (D.I.)								Average Damage Index
	x (+)		x (-)		y (+)		y (-)		
	ID (mm)	D.I.	ID (mm)	D.I.	ID (mm)	D.I.	ID (mm)	D.I.	
No damage	28	0.20	27	0.19	32	0.21	34	0.19	0.20
Minor damage	56	0.41	54	0.39	64	0.42	68	0.37	0.40
Repairable	112	0.82	108	0.78	128	0.83	136	0.75	0.80
Collapse	137	1.00	139	1.00	154	1.00	182	1.00	1.00

The irregularity of the test structure renders the ultimate deformation of the critical story as a variable with the direction, as shown in Table 1. This situation is considered by utilizing the bi-directional plot of the ID (at COM) with damage levels marked in the same plot, as shown in Figure 13. Based on the latter plots, the damage assessments with the conventional damage index which is ID (at COM) in this paper is performed and presented as void bars in Figure 14.

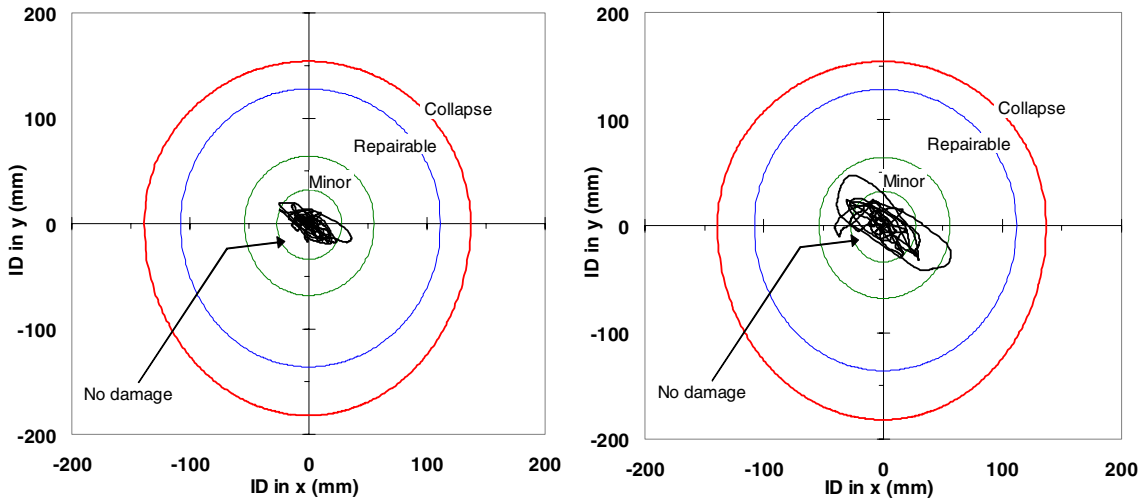

(a) 0.15g PGA (b) 0.20g PGA

Figure 13 Bi-directional plot of ID (at COM) and damage levels

Comparison of the damage assessments by the conventional damage index and the proposed 3D damage index is represented in Figure 14. The difference in damage levels becomes larger as the earthquake intensity goes higher.

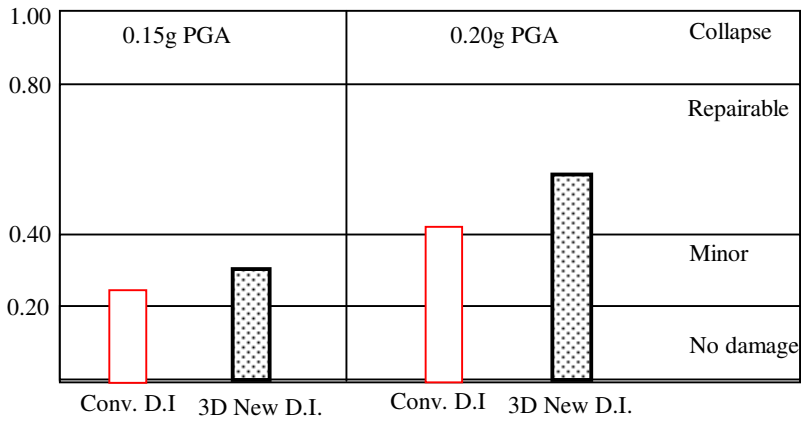

Figure 14 Comparison of damage levels

The visual inspection in Figure 15 shows that the damage was minor after the 0.15g PGA test. However the damage was not the level close to the verge of "No damage" as it was assessed by the conventional damage index in Figure 14. The damage level after 0.20g PGA (Figure 16) is more than "Minor damage" level and extensive spalling and cracking were observed at the flexible edge columns (C1 and C9) as well as the center column (C3) which carries the largest gravity loads. To make a general comment on the comparison, the conventional damage index underestimates the damage level in an increasing manner with the damage level.

(a) C7 (b) C9 (c) C4 (d) C6

Figure 15 Damage after 0.15g PGA test

(a) C1 (b) C9 (c) C3 (d) C6

Figure 16 Damage after 0.20g PGA test

Through the comparison between the damage assessment by damage indices (Figure 14) and visual observations (Figure 15 and Figure 16), it is concluded that damage assessment by the proposed damage index results closer damage level to the real observation than the conventional one.

CONCLUSION

Plan-irregular structures suffer higher levels of earthquake damage than their regular counterparts due to torsional response. This observation lends weight to the necessity of an advanced damage index which provides a quantitative measure of the susceptibility to torsional effects. In this paper, a new damage parameter is derived and shown to be capable of accounting for the effect of torsional imbalance on structural damage. Starting from the concept of planar decomposition of the complex 3D frame, the procedure uses relative weighting of the contribution of each (decomposed) frame line to the overall torsional response. The derived damage parameter, herein terms Demand-to-Capacity Ratio (DCR) is applicable to not only RC frames with planar irregularities but also steel, concrete and composite frames. It is also representative of the torsional sensitivity of moment-resisting and braced frames as well as frame-wall structures. Through an application example, it is demonstrated that the proposed DCR yields convincing results that match damage limit states more accurately than existing indices. Owing to its simplicity and clear application rules, the new damage measure is recommended for use in seismic assessment of structures. While the limit states previously suggested by researchers can be directly used for symmetric cases, their application to structures with planar irregularities should be accompanied with the new damage monitoring methodology suggested in this paper.

ACKNOWLEDGEMENT

The work presented above was undertaken under the Mid-America Earthquake (MAE) Center research project CM-4: Structural Retrofit Strategies, which is part of the Consequence Minimization thrust area. The MAE Center is a National Science Foundation Engineering Research Center (ERC), funded through contract reference NSF Award No. EEC-9701785. The design and detailing of the second case study, the SPEAR building, was provided by the partners of the SPEAR project funded by the European Union. Thanks are due to Professors P.Pinto, M.Fardis, M.Calvi and Drs. E.Carvalho and P.Negro. The cooperation of members of the EU Joint Research Centre, Ispra, is gratefully acknowledged.

REFERENCES

1. Bento R, Azevedo J. "Methodology for the probabilistic assessment of q factors. - A damage index approach." Journal of Earthquake Engineering, 2000; 4(1): 115-139.
2. Williams MS, Sexsmith RG. "Seismic damage indices for concrete structures: a state-of-the-art review." Earthquake Spectra, 1995; 11(2): 319-349.
3. Ghobarah A, Abou-Elfath H, Biddah A. "Response-based damage assessment of structures." Earthquake Engineering and Structural Dynamics, 1999; 28 (1): 79-104.
4. Park YJ, Ang AH-S. "Mechanistic seismic damage model for reinforced concrete." ASCE, Journal of Structural Engineering, 1985; 111(ST4): 722-739.
5. Kappos AJ, Xenos AA. "A reassessment of ductility and energy-based seismic damage indices for reinforced concrete structures." Proceedings of the 3rd European Conference on Structural Dynamics (Eurodyn'96), Florence, Italy, 1996; Vol. 2: 965-970.
6. Park YJ, Ang AH-S. "Seismic damage analysis of reinforced concrete buildings." ASCE, Journal of Structural Engineering, 1985; 111(ST4): 740-757.
7. Park YJ, Ang AH-S, Wen YK. "Damage-limiting a seismic design of buildings." Earthquake Spectra, 1987; 3(1): 1-26.
8. Chung YS, Meyer C, Shinozuka M. "Seismic damage assessment of RC members." Report NCEER-87-0022, National Center for Earthquake Engineering Research, State University of New York at Buffalo, 1987.
9. Chung YS, Meyer C, Shinozuka M. "Automatic seismic design of reinforced concrete building frames." American Concrete Institute Structural Journal, 1990; 87(3): 326-340.
10. Kunnath SK, Reinhorn AM, Park YJ. "Analytical modeling of inelastic seismic response of RC structures." ASCE, Journal of Structural Engineering, 190; 116(4): 996-1017.
11. Kunnath SK, Reinhorn AM, Lobo RF. "IDARC version 3.0: A program for the inelastic damage analysis of RC structures." Technical Report NCEER-92-0022, National Center for Earthquake Engineering Research, State University of New York at Buffalo, New York, 1992.
12. Bracci JM, Reinhorn AM, Mander JB, Kunnath SK. "Deterministic model for seismic damage evaluation of RC structures." Report NCEER-89-0033, National Center for Earthquake Engineering Research, State University of New York at Buffalo, 1989.
13. Roufaiel MSL, Meyer C. "Reliability of concrete frames damaged by earthquakes." ASCE, Journal of Structural Engineering, 1987b; 113(3): 445-457.
14. DiPasquale E, Cakmak AS. "Detection and assessment of seismic structural damage." Report NCEER-87-0015, National Center for Earthquake Engineering Research, State University of New York at Buffalo, 1987.
15. DiPasquale E, Cakmak AS. "Identification of the serviceability limit state and detection of seismic structural damage." Report NCEER-88-0022, National Center for Earthquake Engineering Research, State University of New York at Buffalo, 1988.

16. DiPasquale E, Ju J-W, Askar A, Cakmak AS. “Relation between global damage indices and local stiffness degradation.” ASCE, Journal of Structural Engineering, 1990; 116(5): 1440-1456.
17. Colangelo F. "Experimental evaluztion of member-by-member models and damage indices for infilled rames." Journal of Earthquake Engineering, 2003; 2(4): 569-592.
18. Negro P, Mola E, Molina FJ, Magonette GE. "Full-scale PSD testing of a torsionally unbalanced three-storey non-seismic RC frame." Proceedings of the 13th World Conference on Earthquake Engineering, Vancouver, BC Canada, Aug. 2004; Paper No. 968
19. Molina FJ, Buchet Ph, Magonette GE, Hubert O, Negro P. "Bidirectional pseudodynamic thechnique for testing a three-storey reinforced concrete building." Proceedings of the 13th World Conference on Earthquake Engineering, Vancouver, BC Canada, Aug. 2004; Paper No. 75
20. Jeong S-H, Elnashai AS. "Analytical assessment of an irregular RC full scale 3D test structure." Mid-America Earthquake Center, CD Release 04-03, University of Illinois at Urbana-Chanpaign, 2004.
21. FEMA 356. "Prestandard and Commentary for the Seismic Rehabilitation of Buildings." Federal Emergency Management Agency, 2000.